Probing the Halide Effect in the δ-Bond with One- and Two-Photon Spectroscopy

Jack C. Boettcher,[a,†] Christie Hung,[a,†] Sajeev Kohli,[a,†] Daniel S. Engebretson,[b,*] Daniel R. Morphet,[a] Brandon M. Campbell,[a] Dilek K. Dogutan[a,*] and Daniel G. Nocera[a,*]

[a]*Department of Chemistry and Chemical Biology, Harvard University, 12 Oxford Street, Cambridge, MA 02138, United States.* [b]*Department of Biomedical Engineering, The University of South Dakota, Sioux Falls, SD 57107, United States.*

ABSTRACT: Two electrons in two orbitals give rise to four states. When the orbitals are weakly coupled such as the case for the d_{xy} orbitals of quadruple bond species, two of the states are diradical in character with electrons residing in separate orbitals and two of the states are zwitterionic with electrons paired in one orbital or the other. By measuring one-and two-photon spectra, the one-electron (ΔW) and two-electron (K) energies may be calculated, which are the determinants of the state energies of the four-state model for the two-electron bond. The K energy is thus especially sensitive to the size of the orbital as K is dependent on the distance between electrons. To this end, one- and two-photon spectra of $Mo_2X_4(PMe_3)_4$ are sensitive to secondary bonding interactions of the δ-orbital manifold with the halide orbitals, as reflected in decreasing K energies long the series Cl>Br>I. Additionally, the calculated one-electron energies have been verified with the spectroelectochemical preparation of the $Mo_2X_4(PMe_3)_4^+$ complexes, where the δ bond is a one-electron bond, and K is thus absent. The $\delta \rightarrow \delta^*$ transition shifts by over 10,000 cm^{-1} upon oxidation of $Mo_2X_4(PMe_3)_4$ to $Mo_2X_4(PMe_3)_4^+$, establishing that transitions within the two-electron δ bond are heavily governed by the two-electron exchange energy.

The most prominent and distinguishing element of the discipline of chemistry is the two-electron bond.[1–4] Two electrons, in two atomic orbitals, engenders four states arising from the bonding and antibonding molecular orbitals (φ and φ*, respectively) generated by the linear combination of the two atomic orbitals: $^1\varphi\varphi$, $^3\varphi\varphi^*$, $^1\varphi\varphi^*$, $^1\varphi^*\varphi^*$. The energy ordering of these states, shown in Figure 1, is defined by the one-electron energy ΔW (= E(φ*) – E(φ), the difference between the energies of an electron in a singly occupied φ and φ* orbital) and the two-electron energy K (i.e., the exchange integral).[1] For strongly coupled orbitals, the molecular orbital description of bonding prevails where ΔW >> K and the $^3\varphi\varphi^*$ and $^1\varphi\varphi^*$ lie at ΔW (separated by 2K) and $^1\varphi^*\varphi^*$ occurs at 2ΔW. Conversely, for weakly coupled orbitals, K >> ΔW, valence bond description of bonding prevails where the "biradical" states arising from the $^1\varphi\varphi$ and $^3\varphi\varphi^*$ orbital configurations correspond to one electron in each orbital with spins opposed (singlet) and parallel (triplet) and the "zwitterionic" states arising from the $^1\varphi\varphi^*$ and $^1\varphi^*\varphi^*$ orbital configurations are derived from the antisymmetric and symmetric linear combinations where both electrons are paired in one orbital of either center. Because the "biradical" state arises from a simple spin-flip of an electron in a relatively isolated orbital, the $^3\varphi\varphi^*$ state lies close in energy to the $^1\varphi\varphi$ ground state; in the limit, they are a degenerate ground state. Conversely the "zwitterionic" states are energetically far removed from their diradical counterparts at 2K owing to large two-electron energies that result from pairing electrons in the confined volume of atomic-like orbitals centered on individual metals.

The four-state model of the two-electron bond was recognized at the inception of bonding theories.[1] Heitler and London invoked these states in their description of valence bond theory (VBT)[5] followed by Mulliken's description of these states in the development of molecular orbital theory (MOT).[6] Coulson and

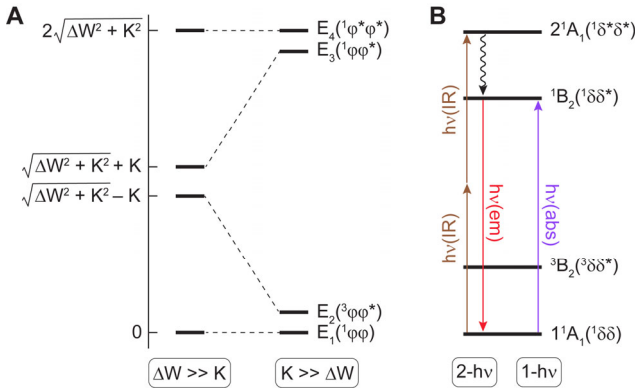

Figure 1. (**A**) Energy level diagram for the four states of two electrons populating the states produced from the linear combination of the bonding (φ) and antibonding (φ*) orbitals formed from two atomic orbitals where ΔW is one-electron energy and K is the two-electron energy comprising the various state transitions. (**B**) Experimental design to determine ΔW and K from one-photon and two-photon spectra. The $^1\delta\delta^*(^1B_2)$ excited state (—) is detected by one-photon absorption spectroscopy. The $^1\delta^*\delta^*(2^1A_1)$ excited state is detected from the fluorescence of the $^1\delta\delta^*(^1B_2)$ excited state (—), which is populated by pumping the $^1\delta^*\delta^*(2^1A_1)$ excited state with two near infrared photons (—) followed by internal conversion.

Fischer unified the four-state model in VBT and MOT with their treatment of stretched hydrogen.[7] Though long recognized the four-state model of the two-electron bond is difficult to experimentally interrogate. For the σ bond, all three excited states ($^3\sigma\sigma^*$, $^1\sigma\sigma^*$ and $^1\sigma^*\sigma^*$) are dissociative.[7,8] In the case of a π bond, all three excited states ($^3\pi\pi^*$, $^1\pi\pi^*$ and $^1\pi^*\pi^*$) are unstable with regard to rotation.[9–11] Conversely, a stable δ-bond formed from d_{xy} orbital overlap is presented by quadruply bonded metal-metal complexes when the

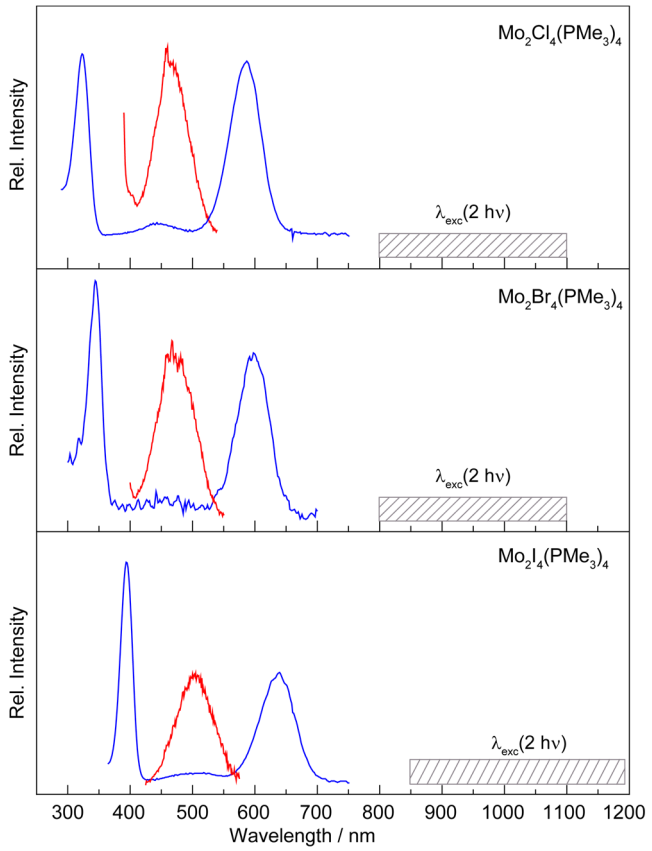

Figure 2. Electronic absorption (—) and two-photon fluorescence excitation spectra (—) for $Mo_2X_4(PMe_3)_4$ complexes in 3-methylpentane at room temperature. The dashed box corresponds to the excitation wavelength region used for the two-photon experiment.

neighboring metal-ligand units are locked by diametrically opposed bulky ligands ($M_2X_4P_4$, P = bulky phosphine, X = halide) or bidentate strapping ligands ($M_2X_4(PP)_2$, (PP) = bidentate bridging phosphine).[12] Moreover, because the δ-bond contributes little to the overall metal-metal bond strength, annihilation of the δ bond upon population of any of the three excited states does little to perturb the metal–metal distance (increases by only ~0.05 Å),[13] and hence to perturb the d_{xy} orbital overlap. The ΔW and K energies may be experimentally determined from one- and two-photon spectroscopy. The $^1\delta\delta(1^1A_1) \rightarrow {}^1\delta\delta^*(^1B_2)$ transition is Laporte and spin-allowed and its energy is offered from UV-visible absorption spectroscopy.[14] The $^1\delta\delta(1^1A_1) \rightarrow {}^1\delta^*\delta^*(2^1A_1)$ transition, which is forbidden by the one-photon selection rules, is allowed by two-photon spectroscopy. From measurement of the one- and two-photon transition energies, ΔW and K may be experimentally defined. These experiments have been undertaken for $M_2X_4P_4$ [15] and Mo_2Cl_4(S,S-dppb)$_2$ (S,S-dppb = S,S-bis(diphenylphosphino)-butane,[16] thus providing the first complete experimental characterization of the two-electron bond in a discrete molecular species. The net result of these studies is that the $^1\delta\delta \rightarrow {}^1\delta\delta^*$ transition energy is largely governed by the two-electron energy, K, and the $^1\delta\delta^*/{}^1\delta^*\delta^*$ excited states possess significant zwitterionic character.

The power of the model shown in Figure 1 is its sensitivity as a measure of covalency versus ionicity in the composition of the two-electron bond. In $Mo_2X_4(PMe_3)_4$ (X = Cl, Br and I) complexes, the reduction potential of these complexes increases along the series Cl < Br < I; this trend, termed "inverse halide order", has been ascribed to greater metal(d_{xy})-halide(p) back-bonding.[17] Such bonding may be probed directly with K, as greater back-bonding should be manifested in a lowering of K due to greater spatial extension of electrons within the orbital. We now report the one- and two-photon spectroscopy of the $Mo_2X_4(PMe_3)_4$ halide series, thus allowing the experimental determination of ΔW and K. We find that K for the d orbital decreases along the "inverse halide order" Cl < Br < I. Moreover, we have prepared the $Mo_2X_4(PMe_3)_4^+$ monocation series by spectroelectrochemistry. With a singly occupied δ orbital, K = 0, thus allowing for an independent measurement of ΔW as compared to that determined from one-and two-photon spectroscopy.

Table 1. Transition Energies[a] within the δ-Manifold of Metal-Metal Complexes

Complex	$^1\delta\delta \rightarrow {}^1\delta\delta^*$	$^1\delta\delta \rightarrow {}^1\delta^*\delta^*$	ΔW	K
$Mo_2Cl_4(PMe_3)_4$	17182	21415	8528	6475
$Mo_2Br_4(PMe_3)_4$	16779	21275	8686	6142
$Mo_2I_4(PMe_3)_4$	15978	19800	7815	6078
	$^2\delta \rightarrow {}^2\delta^*$	ΔΔW[b]		
$Mo_2Cl_4(PMe_3)_4^+$	6906	1622		
$Mo_2Br_4(PMe_3)_4^+$	6766	1920		
$Mo_2I_4(PMe_3)_4^+$	6281	1534		

[a] transition energies in cm^{-1}. [b] ΔΔW is difference between the ΔW energies of corresponding $Mo_2X_4(PMe_3)_4$ and $Mo_2X_4(PMe_3)_4^+$ complexes.

Figure 1B elucidates the experimental design for extracting ΔW and K experimentally. In D_{2d} symmetry, the $^1\delta\delta \rightarrow {}^1\delta\delta^*$ ($1^1A_1 \rightarrow {}^1B_2$) is an allowed one-photon transition. Conversely, whereas the $^1\delta\delta \rightarrow {}^1\delta^*\delta^*$ ($1^1A_1 \rightarrow 2^1A_1$) transition is forbidden by one-photon selection rules, the transition is allowed for two-photon selection rules. Figure 2 shows the one-photon absorption spectrum for $Mo_2X_4(PMe_3)_4$ compounds at room temperature in 3-methylpentane. The well-established $^1\delta\delta \rightarrow {}^1\delta\delta^*$ transition appears as the lowest energy band in UV-vis absorption spectrum (blue line, Figure 2). Though there is no apparent absorption in the 800–1200 nm region of the one-photon spectrum, sample excitation by the Nd:YAG laser in this spectral region results in red emission of the $^1\delta\delta^*$ excited state ($\lambda_{em}(Mo_2X_4(PMe_3)_4)$ = 673, 671 and 715 nm for X = Cl, Br, I[18]). This observation is consistent with excitation into the $2^1A_1(^1\delta^*\delta^*)$ excited state with 2hν absorption, followed by internal conversion to $^1B_2(^1\delta\delta^*)$, from which emission is observed. The two-photon excitation of the fluorescence spectrum is superimposed on the one-photon absorption spectrum shown in Figure 2. The two-photon $^1\delta\delta \rightarrow {}^1\delta^*\delta^*$ ($1^1A_1 \rightarrow 2^1A_1$) assignment is supported by power dependence and polarization measurements. As expected for a two-photon process,[19] the fluorescence intensity varies with the square of the incident laser intensity (Figure S1). Moreover, the polarization ratio (I_{cir}/I_{lin}) is constant and <1.0 across the observed 2hν band (Figure S2); in D_{2d} point group of the $Mo_2X_4(PMe_3)_4$ compounds, a polarization ratio of <1 is expected only for excited states of the same symmetry as the ground state (i.e., A_1).[20]

Table 1 lists the band maxima for the one- and two-photon transition energies. Because the δ bond is not highly perturbed upon population of the δ* orbital, the one- and two-photon band maxima reflect the relative energies of (0.0) transitions of these excited states. From these band maxima, ΔW and K may be evaluated, the

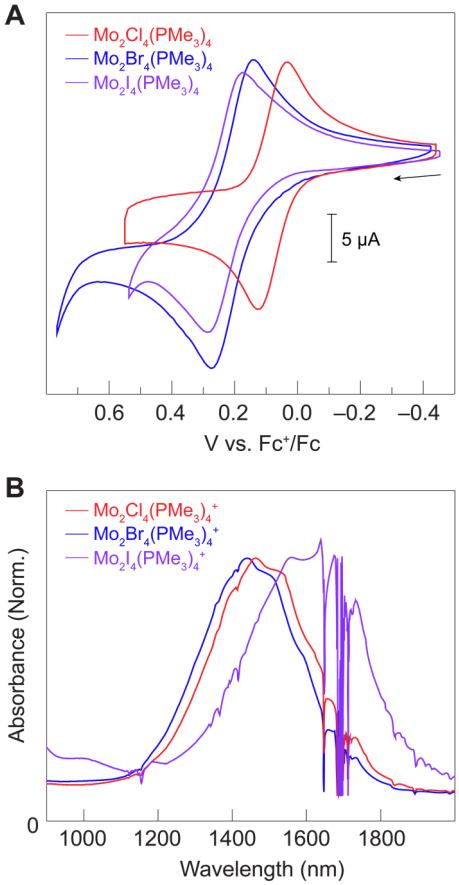

Figure 3. (**A**) Cyclic voltammograms of $Mo_2X_4(PMe_3)_4$ complexes in CH_2Cl_2 with 0.1 M $TBAPF_6$ as the supporting electrolyte. (**B**) UV-visible-NIR absorption spectrum of bulk electrolyzed solutions of $Mo_2X_4(PMe_3)_4$ (E_{appl} = 0.36 V for X = Cl, 0.47 V for X = Br, 0.39 V for X = I).

values of which are listed in Table 1.

A notable prediction of these calculations is that the overlap of the δ–δ* orbital splitting (i.e., ΔW) is small. This has been independently verified by measuring the δ → δ* transition for the oxidized complex, $Mo_2X_4P_4^+$. Here the δ orbital is singly occupied, and therefore the two-electron energy is absent; the δ → δ* transition only reflects ΔW arising from the orbital overlap of d_{xy} orbitals. As reflected by reversibility of the oxidative wave in the cyclic voltammograms of the $Mo_2X_4P_4$ compounds (Figure 3A), the monocation is stable and thus may be generated electrochemically. Figure 3B, shows the UV-visible-NIR spectrum of bulk electrolyzed solutions of $Mo_2X_4(PMe_3)_4$ using an applied potential that is positive of the one-electron oxidation wave. Consistent with the experimentally determined ΔW of the $Mo_2X_4(PMe_3)_4$ compounds, the δ → δ* transition shifts from the visible spectral region to deep in the near-infrared spectral region. The lower ΔW energy of the $Mo_2X_4(PMe_3)_4^+$ complexes as compared to $Mo_2X_4(PMe_3)_4$ reflects the slightly elongated 0.05 Å metal-metal bond increase owing to a half-orbital occupancy of the δ bonding orbital for the monocationic complexes. A slight decrease in the bond strength would be expected to accompany this minor elongation in the metal-metal distance. Of note, the δ bond has been estimated to contribute only 6 kcal mol^{-1} to the overall metal-metal bond strength.[21] The results of Table 1 are consistent with this prediction. The average decrease in ΔW is 1692 cm^{-1} (4.8 kcal mol^{-1}) for the $Mo_2X_4(PMe_3)_4^+$ (δ bond order = ½) as compared to its $Mo_2X_4(PMe_3)_4$ congener (δ bond order = 1).

The value of K monotonically decreases along the series Cl>Br>I. As the two electron energy scales inversely with the distance between electrons ($1/r_{12}$ for electrons e_1 and e_2), this result is consistent with increased metal(d_{xy})-halide(p) back-bonding I>Br>Cl. Consistent with these measurements, *ab inito* calculations on $M_2X_4(PH_3)_4$ complexes suggest a significant amount of halide character mixing with the δ and δ* orbitals.[22] The halogen p-orbitals become energetically more proximate to the metal d-orbitals as the halide electronegativity is decreased, thus accounting for the increased metal(d_{xy})-halide(p) mixing along the series I>Br>Cl. Additional experimental evidence for mixing of halide character into the δ-bond comes from photoelectron spectra[23] and resonance Raman spectra,[24] which shows resonance enhancement when exciting into the δ → δ* transition of $Mo_2X_4(PMe_3)_4$ complexes.

Conclusions

The one- and two-photon spectra of allows the $Mo_2X_4(PMe_3)_4$ halide series allows the one- (ΔW) and two-electron (K) energies of the δ-bond of quadruply bonded complexes to be experimentally determined. We find that K energy decreases along the series Cl>Br>I. As K is dependent on the distance between electrons, K is a sensitive measure of bonding between the d_{xy}(δ) and halide orbital; this bonding interaction increases with descent down the periodic table. The calculated one-electron energies are small, as independently verified with the spectroelectochemical preparation of the $Mo_2I_4(PMe_3)_4^+$ complexes, where the δ bond is a one-electron bond, and K is thus absent. The δ → δ * transition shifts by over 10,000 cm^{-1} upon oxidation of $Mo_2X_4(PMe_3)_4$ to $Mo_2X_4(PMe_3)_4^+$, establishing that transitions within the two-electron δ bond are heavily governed by the two-electron exchange energy.

Experimental Methods

General Methods. All reagents were purchased from commercial suppliers and used without further purification, unless otherwise noted. Dichloromethane was purified by a commercial argon-purged solvent purification system designed by Pure Process Technologies and stored over activated molecular sieves in an N_2-filled glovebox prior to use. 3-Methylpentane was dried over a NaK alloy on a high-vacuum line and vacuum transferred to the spectroscopic cells. The quadruple bond complexes were synthesized according to published procedures for $Mo_2Cl_4(PMe_3)_4$,[25] $Mo_2Br_4(PMe_3)_4$[24] and $Mo_2I_4(PMe_3)_4$.[18] UV-vis-NIR spectra were acquired using a Varian Cary 5000 spectrometer. All electrochemical experiments were performed using a CH Instruments 660C potentiostat in an N_2-filled glovebox. All compounds were dissolved in a dichloromethane solution containing 0.1 M tetrabutylammonium hexafluorophosphate as a supporting electrolyte. A three-electrode setup consisting of a glassy carbon working electrode (x mm diameter), a platinum mesh counter electrode, and a leak-free Ag/AgCl reference electrode (Warner Instruments) was utilized for cyclic voltammetry (CV) measurements. Glassy carbon working electrodes were polished with 1-μm alumina powder on felt prior to use. For each CV, ferrocene was added after the initial measurement to obtain a non-aqueous reference. Bulk-electrolysis was performed in a divided-cell utilizing the three-electrode setup described above except a platinum mesh working electrode was used to maximize current. After each electrolysis, the analyte was sealed in an oven-dried quartz-cuvette for UV-vis-NIR spectroscopy.

TPE Measurements. Two photon experiments were performed with a Coherent Infinity 40-100 Nd:YAG laser (pulse width of 3.5 ns for the 1064 nm fundamental). The pulse energies varied from a few mJ/pulse to 600 mJ/pulse, with a repetition rate to 100 Hz. Wavelength tunability (420 – 710 nm signal frequencies, 710 nm – 2300 nm idler frequencies) was provided by an optical parametric oscillator (OPO) (Coherent Type I XPO). For all of the experiments reported here, the XPO was operated in the idler resonant mode. The XPO was pumped with a constant repetition rate of 100 Hz and pulse energy of 170 mJ/pulse at 354.7 nm. Residual signal energy present with the idler beam was removed by passing the XPO output beam through a Schott RG715 long-wave pass filter. The dependency of emission intensity on incident laser power was accomplished with a 935-10 High Energy Laser Attenuator (Newport Corporation). The exit beam from the attenuator passed through a long focal length (500 mm or 1000cmm) lens to reduce its divergence. The polarization of this beam was manipulated to be either circularly or linearly polarized using a CLPA-10.0-670-1064 Glan-Laser polarizer (GL) (CVI Laser Corporation), a PR-950 double Fresnel rhomb (DFR) (Newport Corporation) and a CVI FR-4-C single Fresnel rhomb (SFR). The GL is used to ensure constant horizontal polarization of the laser beam before it reaches the next two optics. The DFR is placed in a rotatable mount that can be rotated about the optical axis of the laser beam. When the DFR is rotated, the plane of polarization of the laser beam is rotated with respect to the incoming laser beam. This results in changing the plane of polarization of the laser beam with respect to the optical axis of the SFR. The SFR produces either circularly polarized or linearly polarized light, depending on the plane of polarization of the incident laser beam. The laser excitation beam passed through sample onto a J8LP photodetector (Molectron), thermopile detector exhibited a constant wavelength response from 200 nm to 10 μm (±2%) and was fed into a SR250 Gated Integrator/Boxcar Averager Module (Stanford Research Systems) to measure the relative laser intensity. Emission from the $Mo_2X_4(PMe_3)_4$ compounds was dispersed by a SPEX 1681 monochromator and detected by a Hamamatsu R943-02 photomultiplier tube residing in a TE-104 thermoelectrically cooled PMT housing (Products for Research). The output current of the PMT was fed into the 50 Ω load of a Stanford Research Systems SR400 Gated Photon Counter. The discriminator level of the photon counter was adjusted (typically set to –40 mV) to minimize the detection of spurious photons as a result of thermionic emission from the various dynode stages of the PMT. The gate width was 5τ (τ = fluorescence lifetime). For power dependence measurements, the laser energy was adjusted in *c.a.* 10% steps. For polarization dependence measurements, signal intensity for the circular polarization was divided by that measured in the vertical polarizations to yield Ω, the polarization ratio.

ASSOCIATED CONTENT

Supporting Information

Plots of two-photon polarization ratios and power dependences. Supporting Information is available free of charge on the ACS Publications website.

AUTHOR INFORMATION

Corresponding Authors

Dilek K. Dogutan – Department of Chemistry and Chemical Biology, Harvard University, Cambridge, MA 02138, United States; orcid.org/0000-0002-2935-4393 E-mail: dkiper@fas.harvard.edu.

Daniel S. Engebretson – Department of Biomedical Engineering, The University of South Dakota, Sioux Falls, SD 57107, United States; orcid.org/0000-0002-7240-734X; E-mail: Daniel.Engebretson@usd.edu.

Daniel G. Nocera – Department of Chemistry and Chemical Biology, Harvard University, 12 Oxford Street, Cambridge, MA 02138, United States; orcid.org/0000-0001-5055-320X; E-mail: dnocera@fas.harvard.edu.

Authors

Jack C. Boettcher – Department of Chemistry and Chemical Biology, Harvard University, 12 Oxford Street, Cambridge, MA 02138, United States.

Christie Hung – Department of Chemistry and Chemical Biology, Harvard University, 12 Oxford Street, Cambridge, MA 02138, United States.

Sajeev Kohli –Department of Chemistry and Chemical Biology, Harvard University, 12 Oxford Street, Cambridge, MA 02138, United States.

Daniel R. Morphet – Department of Chemistry and Chemical Biology, Harvard University, Cambridge, MA 02138, United States; orcid.org/0000-0002-4179-632X.

Brandon M. Campbell – Department of Chemistry and Chemical Biology, Harvard University, Cambridge, MA 02138, United States; orcid.org/0000-0002-9359-9862.

Notes

The authors declare no competing financial interests.

† JCB, CH and SK contributed equally to this work.

ACKNOWLEDGMENTS

This work was supported by NSF CHE-1855531. DKD acknowledges Harvard University, Department of Chemistry and Chemical Biology.

REFERENCES

1. Cotton F. A.; Nocera, D. G. The whole story of the two-electron bond, with the delta bond as a paradigm, *Acc. Chem. Res.* **2000**, *33*, 483–490.
2. Levine, D. S.; Head-Gordon, M. Clarifying the quantum mechanical origin of the covalent chemical bond, *Nat. Commun.* **2020**, *11*, 4893.
3. Nordholm, S.; Bacskay, G. B. The basics of covalent bonding in terms of energy and dynamics, *Molecules* **2020**, *25*, 2667.
4. Pendás, A. M.; Francisco, E. The role of references and the elusive nature of the chemical bond, *Nat. Commun.* **2022**, *13*, 3327.
5. Heitler, W.; London, F. Wechselwirkung neutraler Atome und homopolare Bindung nach der Quantenmechanik, *Zeit. Phys.* **1927**, *44*, 455-472.
6. Mullliken, R. S. Electronic structures of polyatomic molecules and valence. II. Quantum theory of the double bond, *Phys. Rev.* **1932**, *41*, 751–758.
7. Coulson, C. A.; Fischer, I. XXXIV. Notes on the molecular orbital treatment of the hydrogen molecule, *Philos. Mag.* **1949**, *40*, 386–393.

8. Kolos, W.; Wohiewicz, L. Potential-energy curves for the $X^1\Sigma_g^+$, $b^3\Sigma_u^+$, and $C^1\Pi_u$ states of the hydrogen molecule, *J. Chem. Phys.* **1965**, *43*, 2429–2441.
9. Piotrowiak, P.; Strati, G.; Smirnov, S. N.; Warman, J. M.; Schuddeboom, W. Transient absorption spectra consistent with a $^1\delta^*\delta^*$ excited state of twisted olefins have recently been reported, *J. Am. Chem. Soc.* **1996**, *118*, 8981–8982.
10. Salem, L.; Rowland, C. The electronic properties of diradicals, *Angew. Chem. Int. Ed. Engl.* **1972**, *11*, 92–111.
11. Dauben, W. G.; Salem, L.; Turro, N. J. A classification of photochemical reactions, *Acc. Chem. Res.* **1975**, *8*, 41–54.
12. Cotton, F. A.; Walton, R. A. *Multiple Bonds Between Metal Atoms*, 2nd ed.; Clarendon Press: Oxford, 1993.
13. Collman, J. P.; Garner, J. M.; Hembre, R. T.; Ha, Y. Relative strength of 4d vs 5d δ-bonds: Rotational barriers of isostructural molybdenum and tungsten porphyrin dimers. *J. Am. Chem. Soc.* **1992**, *114*, 1292–1301.
14. Trogler, W. C.; Gray, H. B. Electronic spectra and photochemistry of complexes containing quadruple metal-metal bonds, *Acc. Chem. Res.* **1978**, *11*, 232–239.
15. Engebretson, D. S.; Zaleski, J. M.; Leroi, G. E.; Nocera, D. G. Direct spectroscopic detection of a zwitterionic excited state, *Science* **1994**, *265*, 759–762.
16. Engebretson, D. S.; Graj, E. M.; Leroi, G. E.; Nocera, D. G. Two photon excitation spectrum of a twisted quadruple bond metal-metal complex, *J. Am. Chem. Soc.* **1999**, *121*, 868–869.
17. Zietlow, T. C.; Hopkins, M. D.; Gray, H. B. Electrochemistry of quadruply bonded molybdenum dimers. Evidence for metal-to-halide back-bonding, *J. Am. Chem. Soc*. **1986**, *108*, 8266–8267.
18. Hopkins, M. D.; Gray, H. B. Nature of the emissive excited state of quadruply bonded $Mo_2X_4(PMe_3)_4$ complexes, *J. Am. Chem. Soc.* **1984**, *106*, 2468–2469.
19. Lin, S. H.; Fujimura, Y.; Neusser, H. J.; Schlag, E. W. *Multiphoton Spectroscopy*; Academic Press: Orlando, FL, 1984.
20. Nasciemento, M. A. The polarization dependence of two-photon absorption rates for randomly oriented molecules, *Chem. Phys.* **1983**, *74*, 51–66.
21. Smith, D. C.; Goddard III, W. A. Bond energy and other properties of the rhenium-rhenium quadruple bond, *J. Am. Chem. Soc.* **1987**, *109*, 5580–5583.
22. Milletti, M. C. Theoretical study of the influence of the halide ligands on the metal–metal quadruple bond in the $M_2X_4(PH_3)_4$ (M = Mo, W; X = Br, Cl, I) series of complexes, *Polyhedron* **1993**, *12*, 401–405.
23. Cotton, F. A.; Hubbard, J. L.; Lichtenberger, D. L.; Shim, I. Comparative studies of Mo–Mo and W–W quadruple bonds by SCF-Xα-SW calculations and photoelectron spectroscopy, *J. Am. Chem. Soc.* **1982**, *104*, 679–686.
24. Hopkins, M. D., Schaefer, W. P., Bronikowski, M. J., Woodruff, W. H., Miskowski, V. M., Dallinger, R. F., Gray, H. B. Ligand perturbation of the molecular and electronic structures of quadruply bonded dimers. The crystal structures of $Mo_2Br_4(PMe_3)_4$ and $Mo_2I_4(PMe_3)_4$, and the vibrational and electronic spectra of a series of $M_2X_4L_4$ complexes, *J. Am. Chem. Soc.* **1987**, *109*, 408–416.
25. Cotton, F. A.; Extine, M. W.; Felthouse, T. R.; Kolthammer, B. W.; Lay, D. G. Molecular and electronic structures of two quadruply bonded ditungsten compounds and a dimolybdenum homolog, *J. Am. Chem. Soc.* **1981**, *103*, 4040–4045.

TOC